

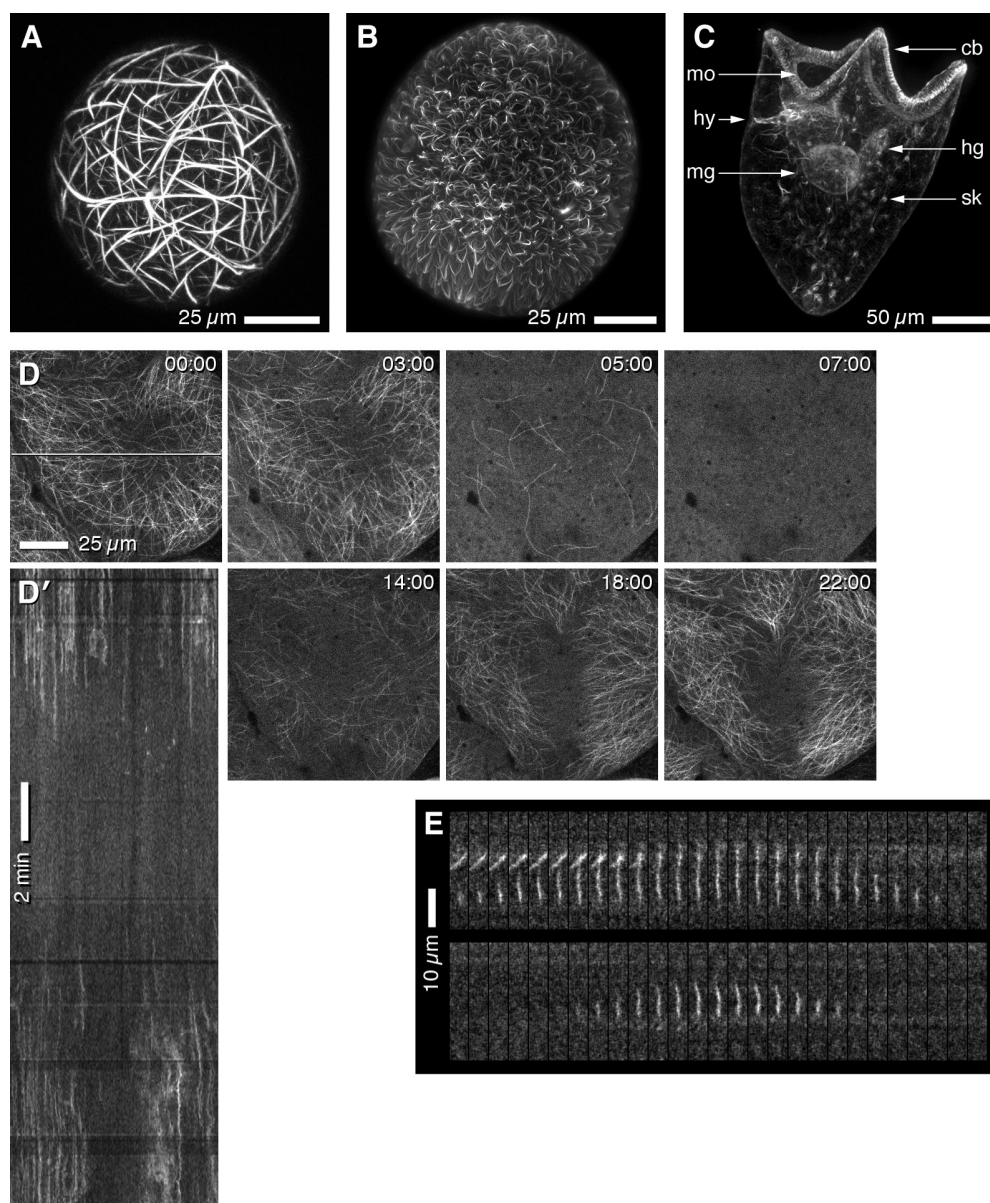
von Dassow et al., <http://www.jcb.org/cgi/content/full/jcb.200907090/DC1>

Figure S1. **Moderate expression of EMTB-3G does not interfere with mitosis or morphogenesis.** (A) Purple urchin zygote injected to ~2% egg volume with high concentration (1 ng/nl; >10× normal imaging concentration) EMTB-3G mRNA arrests as a zygote with highly stable microtubule bundles. (B) Projection of 68 0.5-μm confocal sections through a 30-h-old purple urchin embryo at the mesenchyme blastula stage from a zygote injected to ~2% egg volume with normal imaging concentration (0.05 ng/nl) EMTB-3G mRNA. Uniform cell size and consistent apical-basal orientation indicate the scarcity of mitotic or developmental errors. (C) Projection of 44 2-μm sections through a 4-d-old purple urchin pluteus larva, compressed between slide and coverslip to trap it, from the same batch of injected eggs as B. Morphogenesis and relative proportions of ciliated band (cb), skeleton (sk), digestive tract (mo, mouth; mg, midgut; hg, hindgut), and coeloms (hy, hydropore) are all normal. (D) Single superficial sections from a 6 h *X. laevis* embryo (EMTB-3G; Video 2). (D') Kymograph from single-pixel strip shown in the 00:00 frame of D; as in urchins (Fig. 2), long streaks (kinematically stable microtubules) appear before furrowing, mostly outside the equator. Time is shown in minutes:seconds. (E) Successive frames showing cortical microtubules growing and shrinking (3 s intervals); enlargement from a *X. laevis* blastomere expressing EMTB-3G (intensities squared to enhance contrast).

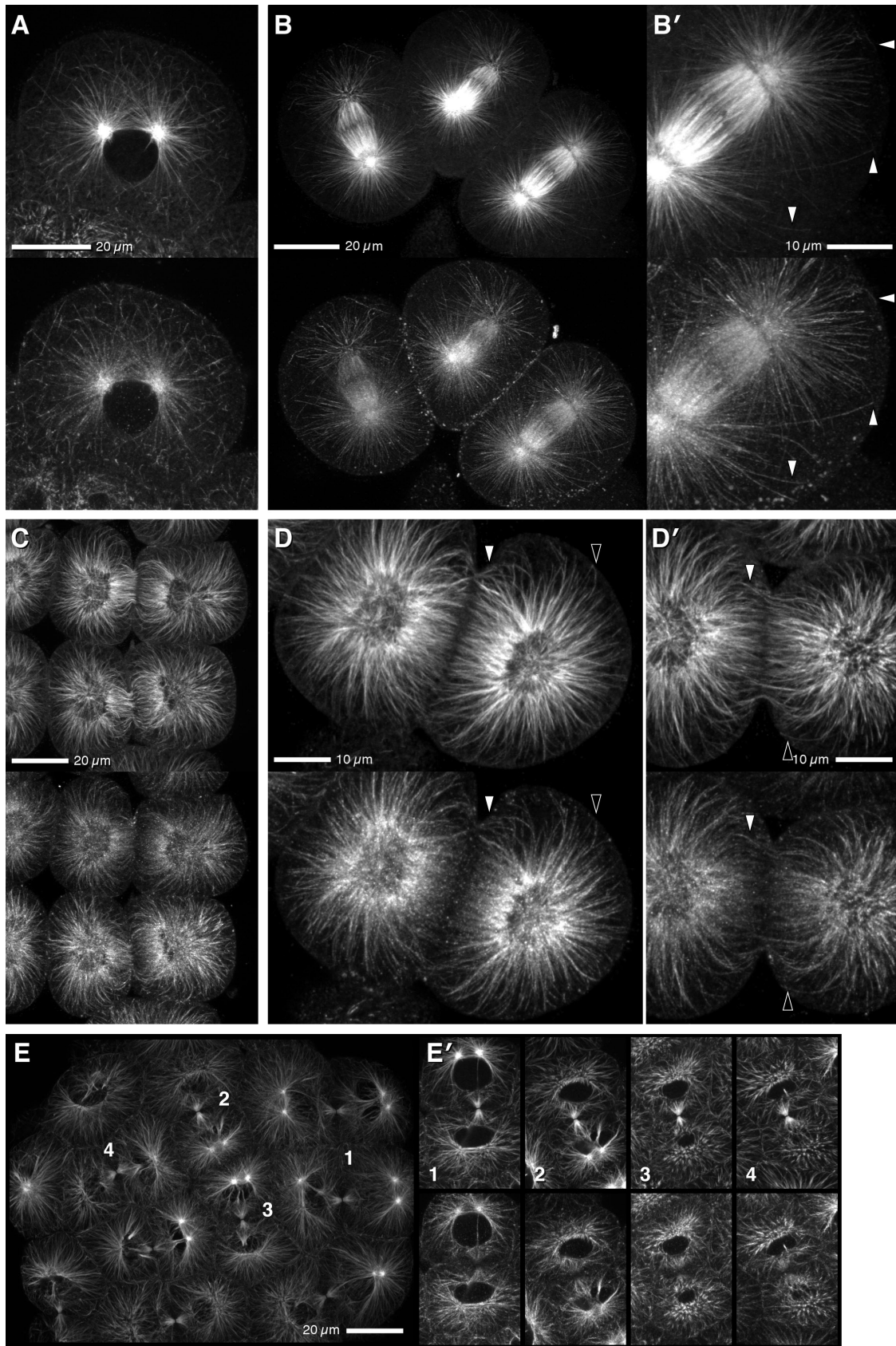


Figure S2. **EMTB-3G colocalizes with microtubules labeled by immunofluorescence.** Sand dollar eggs were injected with <0.05 ng/nl EMTB-3G mRNA, then fixed and labeled with anti-tubulin (top) and anti-GFP (bottom) antibodies. (A) An interphase cell; projection of five $0.3\text{-}\mu\text{m}$ sections. (B and B') A trio of anaphase cells; projection of 46 $0.25\text{-}\mu\text{m}$ sections. B' shows a 2x enlarged view. Astral microtubules are equally labeled by anti-GFP and anti-tubulin. Note the accurate labeling of apparently single astral microtubules by EMTB-3G (B', arrowheads). (C and C') Telophase; projection of five $0.5\text{-}\mu\text{m}$ confocal

sections. Astral microtubules that are collected together by the cleavage furrow, destined for the central spindle, are accurately labeled by EMTB-3G. Midzone microtubules, however, are relatively underlabeled. (D and D') Two telophase cells from the same embryo; projection of five 0.5- μ m confocal sections. Similar to C and C', astral microtubules gathered together by the ingressing furrow, which will contribute to the midbody, are labeled accurately by EMTB-3G (closed arrowheads), but the midzone of the central spindle is relatively poorly labeled. Open arrowheads point out close correspondence of both labels for astral microtubule ends outside the furrow. (E and E') Complete cytokinesis. E is a projection of 22 0.5- μ m confocal sections (anti-tubulin only), whereas each vertical pair in E' is a projection of the three sections that include the midbody for each of four cell pairs in E (numbered). The midbody is the brightest object recognized by anti-tubulin besides the centrosomes themselves (E', top); although most of the midbody is labeled by EMTB-3G (E', bottom), the very middle is absent, and the midbody as a whole is less brightly labeled than the rest of the microtubule array.

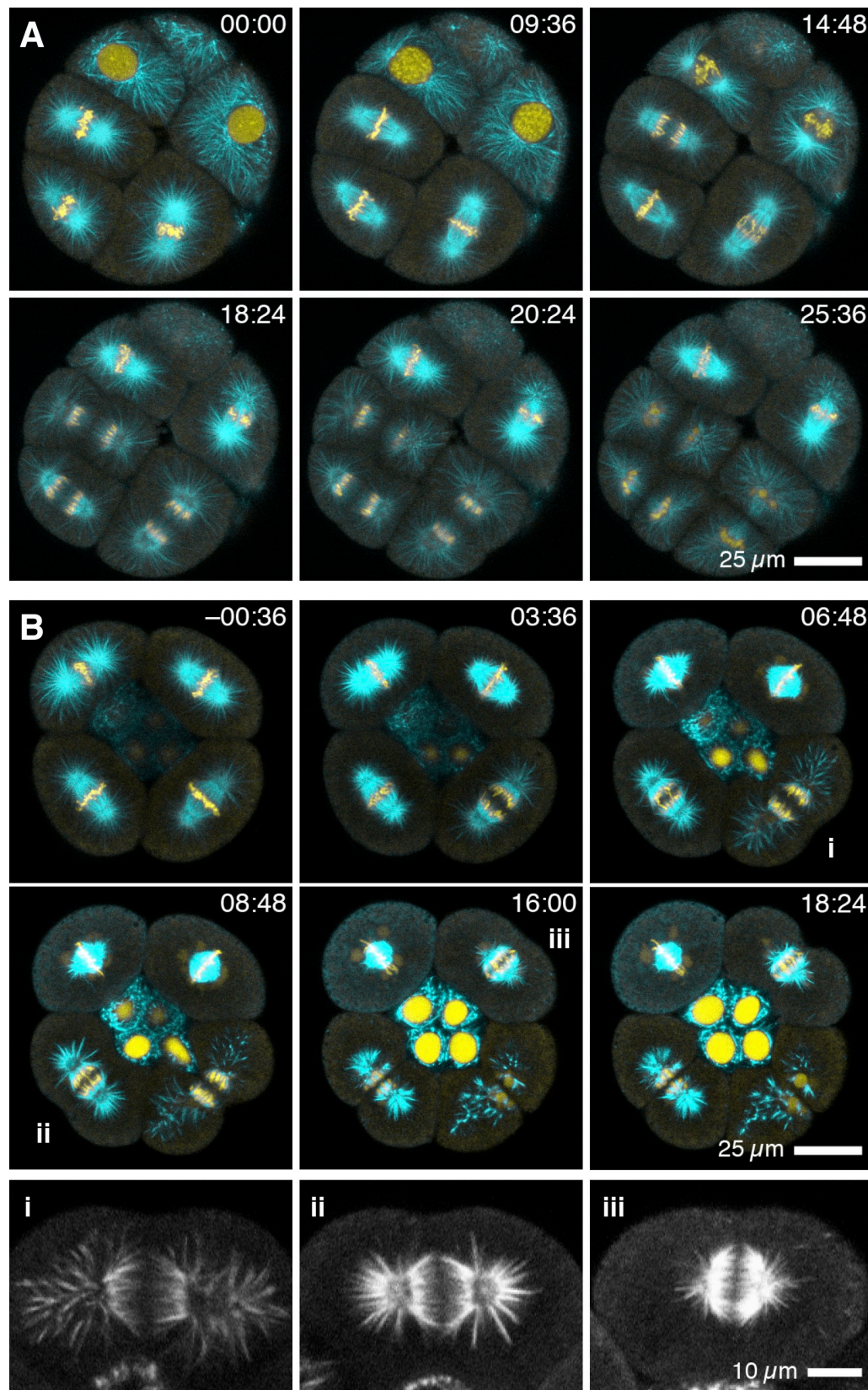


Figure S3. **Accurate cleavage between separating chromatids in control and TSA-treated cells.** Single confocal sections. Cyan, EMTB-3G; yellow, mC-H2B (see Video 5). (A) Untreated 16-cell purple urchin embryo, side view, epitomizing normal correlation between aster development, furrowing, and the extent of separation of sister chromatids. (B) 16-cell purple urchin embryo; 15 μ M TSA was added at time 00:00. Because of a slight asynchrony in mitosis at the time of TSA addition, each macromere exhibits a distinct phenotype: the northwest cell has not quite achieved chromosome alignment at the time of TSA addition, and remained in metaphase. Cells that cleaved are shown as 2 \times enlargements (i–iii). The southeast cell (i) entered anaphase shortly after TSA addition; this cell retained substantial asters with rays that approach, if not reach, the cell surface, and separated sister chromatids significantly. The southwest cell (ii) entered anaphase \sim 5 min after TSA addition; asters are present but much reduced and do not reach the cortex, and chromatid separation is limited. The northeast cell (iii) entered anaphase 10–12 min after TSA addition, and has both minimal asters and minimal chromatid separation. All three cells that entered anaphase, however, despite differences in aster extent and sister chromatid separation, initiated furrowing at the appropriate position and time after anaphase onset.

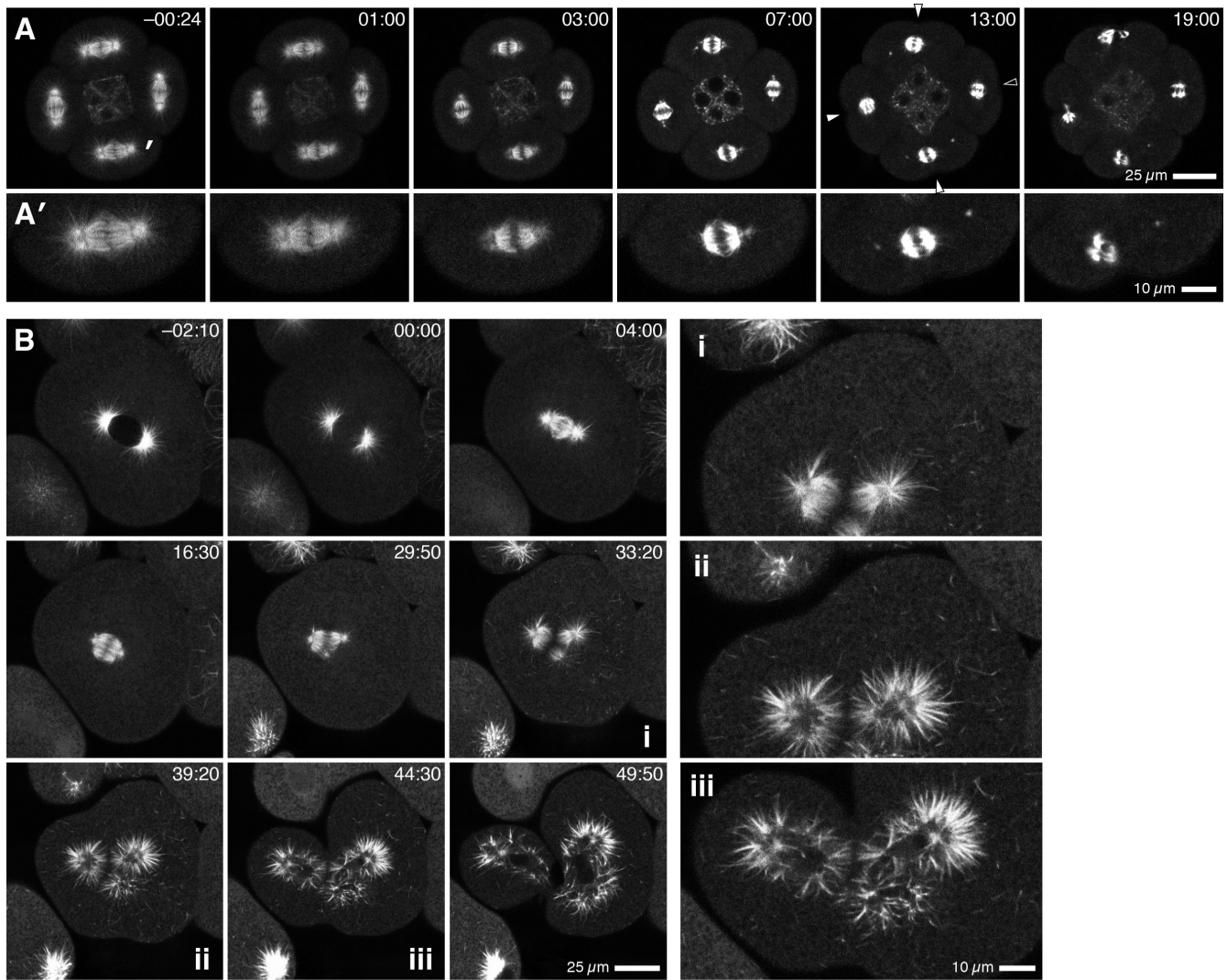


Figure S4. Cleavage occurs even after extreme or prolonged loss of astral microtubules. Single confocal sections; EMTB-3G. (A and A') 16-cell purple urchin embryo treated with 40 μ M TSA at time 00:00; A' shows a 2x enlarged view of the southern cell (indicated by the white mark). All four cells entered anaphase, but extremely reduced spindle length with a very small midzone gap suggests minimal chromatid separation (compare with similar cases in Fig. 5). Virtually no astral microtubules survived, and some centrosomes separated from the spindle (bright dots in the 13:00 frame). Nonetheless, all cells initiated furrows at the right place (arrowheads, 13:00), only one of which regressed (open arrowheads), whereas the other three of the four completed (19:00). (B) One of eight cells in a slightly compressed sand dollar embryo treated with 20 μ M TSA at time 00:00, before nuclear envelope breakdown. After an exceptionally long metaphase (>20 min) with no long astral microtubules, and during which one half of the spindle bifurcated, this cell entered anaphase \sim 26 min after TSA addition. Some astral microtubules regrew in anaphase, but none approach within 10 μ m of the cortex. 2x enlarged views in i–iii show the half of the cell on which the furrow appears first. Furrowing began, as in normal cells, around the time that chromosomes began to decondense, forming vesicles near centrosomes (39:20). Despite obvious derangement of the mitotic apparatus and a long delay, the furrow successfully partitioned daughter nuclei. Video 4 includes A and B. Time is shown in minutes:seconds.

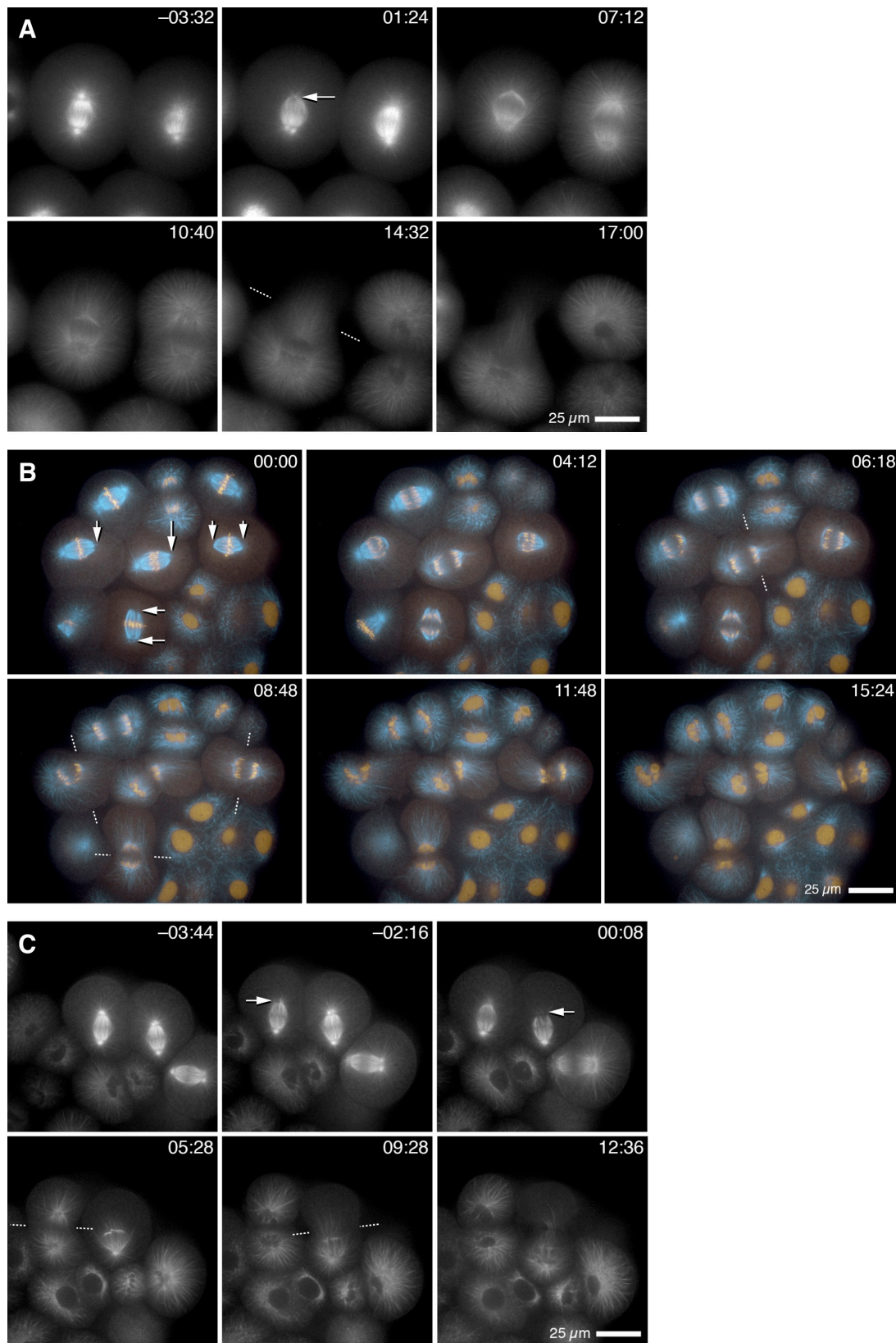
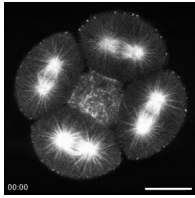
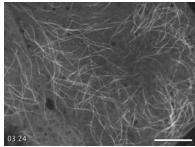


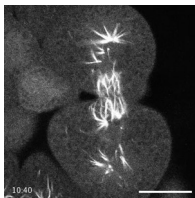
Figure S5. **Additional cases of centrosome ablation.** Single-plane recordings of sand dollar embryos; times are given in minutes:seconds after the end of irradiation. Arrows, ablated centrosome; dotted lines, cleavage plane. (A) An extreme single-pole ablation: virtually no astral microtubules remain in the ablated pole, and the ablated spindle half shrivels. Furrowing occurs beyond the ablated end of the mitotic spindle. See Video 7. (B) Mix of normal, two singly ablated, and two doubly ablated cells in an embryo (cyan, EMTB-3G; yellow, mC-H2B) showing chromosome segregation despite pole ablation. Both singly ablated cells exhibit shifts of the furrow toward the ablated pole, although in one cell, a correction makes the furrow partition chromosomes. Both doubly ablated cells make broad furrows; those furrows cross the spindle midzone, but in one cell, the chromosomes are not separated enough to be accurately partitioned (see Video 8). (C) Two single-pole ablations, contrasting a cell with substantial astral regrowth with a cell in which ablation is more complete. All three mitotic cells shown here were preparing to divide unequally, probably representing delayed micromere formation in this 32-cell embryo. The left cell redevelops the ablated aster, and cleavage proceeds with only a subtle shift of furrow relative to midzone. The middle cell retains no aster around the ablated pole, and the furrow forms and passes beyond the remains of the mitotic apparatus.



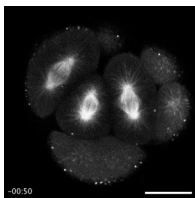
Video 1. **Ensconsin-3xGFP in normal urchin embryos.** The three sequences correspond to Fig. 1 (A–C). All are time-lapse sequences of single confocal sections (Radiance 2000; Bio-Rad Laboratories). First segment, purple urchin 16-cell embryo; second segment, sand dollar 28-cell embryo; third segment, sand dollar eight-cell embryo. Real times are indicated, and the video is encoded at 15 frames/s. Bars, 25 μ m.



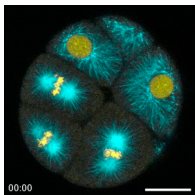
Video 2. **Ensconsin-3xGFP in a normal *X. laevis* blastomere.** The video corresponds to Fig. S1 D: time-lapse sequence of single superficial confocal section (MRC1024; Bio-Rad Laboratories). Real times are indicated, and the video is encoded at 15 frames/s. Bar, 25 μ m



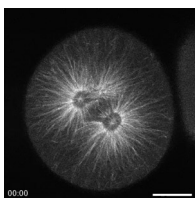
Video 3. **Urchin embryos expressing ensconsin-3xGFP treated with nocodazole at anaphase.** Time-lapse sequences of single confocal sections (Radiance 2000; Bio-Rad Laboratories). First segment (Fig. 3 A), eight-cell purple urchin embryo treated with 20 μ M nocodazole at time 00:00. Second segment (no corresponding figure), eight-cell purple urchin embryo treated with 20 μ M nocodazole at time 00:00. Third segment (Fig. 3 B), 16-cell purple urchin embryo treated with 10 μ M nocodazole at time 00:00. Fourth segment (Fig. 3 C), 16-cell sand dollar embryo treated with 10 μ M nocodazole at time 00:00. Fifth segment (Fig. 3 C), enlarged view of eastern cell from previous segment. Real times are indicated, and the video is encoded at 15 frames/s. Bars, 25 μ m.



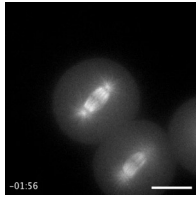
Video 4. **Urchin embryos expressing ensconsin-3xGFP treated with TSA.** Time-lapse sequences of single confocal sections (Radiance 2000; Bio-Rad Laboratories). First segment (Fig. 4 A), 16-cell purple urchin embryo treated with 20 μ M TSA at time 00:00. Second segment (Fig. 4 C), one cell within a 16-cell sand dollar embryo treated with 25 μ M TSA 10 min before time 00:00. Third segment (Fig. S4 A), 16-cell purple urchin embryo treated with 40 μ M TSA at time 00:00. Fourth segment (Fig. S4 B), one cell in an eight-cell sand dollar embryo treated with 20 μ M TSA at time 00:00. Real times are indicated, and the video is encoded at 15 frames/s. Bars, 25 μ m



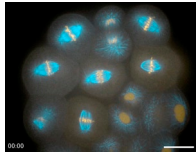
Video 5. **Urchin embryos coexpressing ensconsin-3xGFP and mC-H2B, normal versus TSA treated.** Time-lapse sequences of single confocal sections (Radiance 2000; Bio-Rad Laboratories) with EMTB-3G (microtubules) in shown cyan and mC-H2B (chromatin) in yellow. First segment (Fig. S3 A), untreated 16-cell purple urchin embryo. Second segment: (Fig. S3 B), 16-cell purple urchin embryo treated with 15 μ M TSA at time 00:00. Real times are indicated, and the video is encoded at 15 frames/s. Bars, 25 μ m.



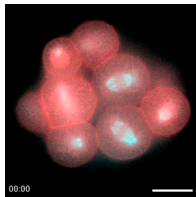
Video 6. **Anucleate sand dollar cytoplasts expressing ensconsin-3xGFP.** Time-lapse sequences of single confocal sections (Radiance 2000; Bio-Rad Laboratories). Three segments correspond to Fig. 7 (A–C). Real times are indicated, and the video is encoded at 15 frames/s. Bars, 25 μ m.



Video 7. Ablation of single centrosomes in sand dollar blastomeres expressing ensconsin-3xGFP. Time-lapse sequences of single confocal sections (CARV; BD). The first segment corresponds to Fig. 8 A, the second segment is a similar case for which there is no corresponding figure, and the third segment corresponds to Fig. S5A. Real times are indicated, and the video is encoded at 15 frames/s. Bars, 25 μ m.



Video 8. Single and double centrosome ablations in a sand dollar embryo coexpressing ensconsin-3xGFP (cyan) and mC-H2B (yellow). Time-lapse sequence of single confocal sections (CARV; BD). Video corresponds to Fig. S5 B. Real times are indicated, and the video is encoded at 15 frames/s. Bar, 25 μ m.



Video 9. Centrosome ablation in sand dollar blastomeres coexpressing GFP-rGBD (red) and ensconsin-3xGFP (cyan). Time-lapse sequences of single confocal sections (CARV; BD). First segment (Fig. 8 B): two single ablations surrounded by normal cells. Second segment (Fig. 8 D): one normal, one singly ablated, and one doubly ablated cell. Third segment (Fig. 8 C): doubly ablated cell. Real times are indicated, and the video is encoded at 15 frames/s. Bars, 25 μ m.